

JAERI-M

9 7 4 7

PRELIMINARY DESIGN OF  
FUSION REACTOR FUEL CLEANUP SYSTEM  
BY PALLADIUM ALLOY MEMBRANE METHOD

October 1981

Hiroshi YOSHIDA, Satoshi KONISHI  
and Yuji NARUSE

この報告書は、日本原子力研究所が JAERI-M レポートとして、不定期に刊行している研究報告書です。入手、複製などのお問い合わせは、日本原子力研究所技術情報部（茨城県那珂郡東海村）あて、お申しこしてください。

JAERI-M reports, issued irregularly, describe the results of research works carried out in JAERI. Inquiries about the availability of reports and their reproduction should be addressed to Division of Technical Information, Japan Atomic Energy Research Institute, Tokai-mura, Naka-gun, Ibaraki-ken, Japan.

PRELIMINARY DESIGN OF  
FUSION REACTOR FUEL CLEANUP SYSTEM  
BY PALLADIUM ALLOY MEMBRANE METHOD

Hiroshi YOSHIDA, Satoshi KONISHI  
and Yuji NARUSE

Division of Thermonuclear Fusion Research,  
Tokai Research Establishment, JAERI

(Received September 22, 1981)

A design of palladium diffuser and Fuel Cleanup System (FCU) for D-T fusion reactor is proposed. Feasibility of palladium alloy membrane method is discussed based on the early studies by the authors. Operating conditions of the palladium diffuser are determined experimentally. Dimensions of the diffuser are estimated from computer simulation. FCU system is designed under the feed conditions of Tritium Systems Test Assembly (TSTA) at Los Alamos Scientific Laboratory. The system is composed of Pd-diffusers, catalytic oxidizer, freezer and zinc beds, and has some advantages in system layout and operation. This design can readily be extended to other conditions of plasma exhaust gases.

Keywords ; Fusion Reactor Fuel Cycle, Fuel Purification  
System, Tritium, Hydrogen Isotopes, Impurities,  
Palladium Diffuser, Hot Metal Getter, Cryogenic  
Adsorption Bed, Catalytic Oxidiser, System Design

パラジウム合金膜法による核融合炉  
燃料精製系の予備的検討

日本原子力研究所東海研究所核融合研究部

吉田 浩・小西哲之・成瀬雄二

(1981年9月22日受理)

D-T核融合炉の燃料循環系を対象としたパラジウム拡散器およびこれを用いた燃料精製システム (Fuel Cleanup System) に関する予備的な設計を行なった。

パラジウム合金膜法の適用性は、筆者らの既往研究に基づいて検討した。パラジウム拡散器の操作条件は実験により決定し、その形状・大きさはコンピューター計算に基づいて設定した。

精製システムの設計は、Los Alamos Scientific Laboratory の Tritium Systems Test Assembly (TSTA) における、供給ガス条件に従った。

本システムの必要機器は、パラジウム拡散器、触媒酸化反応器、低温トラップ、鉅鉛ベッド、真空ポンプなどであり、システム構成および操作条件において幾つかの利点が挙げられる。なお、この設計は、容易に他のD-T炉燃料排ガス条件に拡張することができる。

## Contents

1.	Introduction .....	1
2.	Experimentals .....	2
2.1	Apparatus .....	2
2.2	Basic permeation characteristics .....	3
2.3	Chemical reactions in permeation cell ....	4
2.4	Effects of impurities .....	5
2.5	Effects of thermal cycling .....	6
3.	Design of palladium diffuser .....	8
3.1	Operating conditions of diffuser .....	8
3.2	Analysis of separation characteristics ...	9
3.3	Specifications of diffuser .....	12
4.	Description of Fuel Cleanup System(FCU) ..	13
4.1	FCU system in TSTA .....	13
4.2	Alternative FCU system with Pd-diffuser ..	14
	(1) D-T reactor exhaust gases .....	14
	(2) Process description .....	15
5.	Conclusion .....	17
	Acknowledgement .....	18
	References .....	18

## 1. Introduction

In an exhaust gas of D-T fusion reactor, various impurities such as  $(D,T)_2O$ ,  $N(D,T)_3$ ,  $C(D,T)_4$ ,  $O_2$ ,  $N_2$ ,  $CO$ ,  $CO_2$ , Ar and He will be included. Therefore, purification processes of hydrogen isotopes are necessary for a pretreating process of hydrogen isotope separation in fuel circulation system of fusion reactor<sup>(1)-(3)</sup>.

Palladium alloy membrane method, which makes use of the selective permeability for hydrogen isotopes, is supposed to be attractive one because of its simplicity, handling ease in continuous operation and production of hyper pure hydrogen<sup>(4)</sup>. However, it had not been considered as a feasible technique due to the assumed difficulties as follows ; weakening by thermal cycling and hydrogen embrittlement, poisoning by impurities, need of elevated pressure and temperature, and need for multi-stage separation system to obtain high recovery efficiency of tritium<sup>(3)</sup>. Owing to recent development of fabrication technology of multi-components palladium alloys and their fine tubes, palladium membrane becomes to have high resistivity against thermal cycling and hydrogen embrittlement<sup>(4)</sup>.

In the present work, experiments were performed on effects of impurities and thermal cycling with a commercial Pd-Ag(+Au+Ru) alloy to study the feasibility of membrane.

Computer calculations on hydrogen recovery with tube-type diffuser were done under practicable operation conditions at moderate pressure and temperature.

Based on these results, preliminary design of fuel clean-up system was studied.

## 2. Experimentals

### 2.1 Apparatus

A conceptual flow sheet of the experimental apparatus and detail structure of permeation cell are shown in Figure 1 and Figure 2, respectively. Feed gas flowing into the permeation cell is preheated before it reaches the outer surface of the permeation tube. Feed pressure is regulated by control valve CV-1 and measured by Bourdon tube pressure gauge PG-1 (measuring range; 0 - 2000kPa, precision; 0.1% of full scale). Feed flow rate is measured by mass flow meter FIR-1 (measuring range; 0 - 100std.cm<sup>3</sup>.H<sub>2</sub>/min, precision; 1% of full scale).

Permeated and unpermeated gas (bleed gas) leaving the cell are cooled to room temperature by cooling coils HX-1, 2, and their pressures and flow rates are measured by Bourdon tube pressure gauges PG-2, 3 (0 - 1000kPa, 0.1%F.S.) and mass flow meters FIR-2, 3, respectively. Control valves CV-2, 3 are used to regulate the pressures. Permeation temperature is measured with six sets of thermocouple, they are welded on the surface of the outer shell of the permeation cell.

Swage locks and brazing connections were used to joint all parts of the apparatus to keep the leak rate lower than  $1 \times 10^{-6}$  atm.cm<sup>3</sup>.He/sec.

The permeation cell is constructed with an outer shell (16mm outer diameter, 12mm inner diameter, 370mm long, SUS316), an inner shell (6mm outer diameter, 4mm inner diameter, 314mm long, SUS316), palladium alloy tube (1.6mm outer diameter,  $8 \times 10^{-3}$  cm thickness, 96.7mm effective length) and others.

The end of the permeation tube is sealed, and the other end is brazed to nickel tube (2.03mm outer diameter, 103mm long).

Nominal content of silver in the palladium alloy is about 25%, whereas a certain amounts of gold and ruthenium are assumed to contain.

## 2.2 Basic permeation characteristics<sup>(5)</sup>

In the experiments, basic permeation characteristics, that is, pressure and temperature dependence of permeation flux, permeation coefficient, diffusion coefficient and isotope effect, were measured with the permeation cell.

Figure 3 shows a typical experimental result. In the Figure, permeation fluxes for  $H_2$  and  $D_2$  obtained at various temperatures were shown against square root pressure difference. Here,  $P_h$  and  $P_l$  are the driving and back pressures in the cell, respectively. Most of the data at each temperature lie on straight-lines, indicating that Sieverts' law are held in the experimental range. The slope, which is equivalent to permeation coefficient, increases with the increase of the temperature. Arrhenius relation between the permeation coefficient and temperature was also observed. From these experimental results, following experimental equations were determined by least square method.

$$Q_H = 7.31 \times 10^{-7} \exp \left[ -\frac{1370}{RT} \right] \quad (\text{mol.cm/cm}^2.\text{min.kPa}^{1/2})$$

$$Q_D = 4.78 \times 10^{-7} \exp \left[ -\frac{1470}{RT} \right] \quad ( \quad " \quad )$$

where,  $Q_H$  and  $Q_D$  are the permeation coefficients for  $H_2$  and  $D_2$ , respectively.

### 2.3 Chemical reactions in permeation cell

The permeation cell was assembled with palladium alloy membrane tube, nickel tube and stainless steel tube. These structural materials are considered to have catalytic activity for gases such as  $H_2$ ,  $O_2$ ,  $NH_3$ ,  $CH_4$ ,  $CO$  and so on.

Chemical reactions in the cell were examined with  $H_2$ -1.02%  $NH_3$  and  $H_2$ -0.1% $O_2$ -0.105% $CH_4$  systems. Table 1 summarizes the experimental conditions, and analytical results of bleed gases and the composition of feed gases. In each run, flow ratio of feed to bleed was changed from 2 to 8 under constant temperature (707K). Gas analysis was done by means of TCD type gas chromatograph.

Precision of quantitative analysis of ammonia is not so good because of its high condensibility. However, runs (I-1 - 3) show that concentration of ammonia in bleed gas is roughly proportional to the flow ratio. In runs (I-4 - 7), concentration of nitrogen increases with decreasing of gas velocity in the permeation cell. The experimental result indicate that catalytic decomposition of ammonia, that is  $2NH_3 \rightleftharpoons N_2 + 3H_2$ , proceeds on the surface of the metals. In respect to tritium recovery from tritiated ammonia, this reaction is favorable.

With the  $H_2$ - $O_2$ - $CH_4$  system (Run I-8,9), concentration of oxygen is markedly reduced without producing carbon mono-oxide. Due to the adsorption-desorption characteristics of column packing (molecular sieve-5A) of gas chromatograph, water vapor and carbon-dioxide could be measured. However,

oxidation of methane such as  $\text{CH}_4 + 2\text{O}_2 \rightleftharpoons \text{CO}_2 + 2\text{H}_2\text{O}$  or  $\text{CH}_4 + 1/2 \text{O}_2 \rightleftharpoons \text{CO} + \text{H}_2$  are assumed to be improbable because of high catalytic activity of palladium for the reaction  $2\text{H}_2 + \text{O}_2 \rightleftharpoons 2\text{H}_2\text{O}$ .

#### 2.4 Effects of impurities

Many species of impurities are assumed to be included in fusion reactor exhaust gases. The estimated species are  $\text{O}_2$ ,  $\text{NH}_3$ ,  $\text{CH}_4$ ,  $\text{CO}$ ,  $\text{CO}_2$ ,  $\text{H}_2\text{O}$  and inert gases (He, Ar) (1)-(3).

These impurities should be removed to ensure efficient and safe operation of cryogenic distillation system (hydrogen isotope separation process).

In the experiments, effects of these impurities, which are considered to be poisonous for palladium alloy membrane were examined. The experimental conditions were as follows, driving pressure; 120 - 1500kPa, temperature; 653 - 853K, concentrations of impurities; 10 - 10000ppm. Effects of high temperature exposure to methane gas and vacuum oil vapor were also examined.

Figure 4 - 6 and Table 1 show typical experimental results. In the Figure 4, it is apparent that decrease of the permeation flow rate did not occur during operation (about 24hrs). Steady state flow rates for  $\text{H}_2$ -1.02% $\text{NH}_3$  system and  $\text{H}_2$ -0.1% $\text{O}_2$ -0.105% $\text{CH}_4$  system were equivalent to about 97% of that for pure hydrogen. The result was based on the difference of hydrogen partial pressure in the cell.

Table 2 summarizes the experimental conditions and the

effects of methane gas exposure. The exposure was performed at high temperature( 709 - 823K ) and high pressure( 134 - 382kPa). Whole time of the exposure was 120hrs. As seen in the Figure 5, Sieverts' law was held for run(M-4) and no hysteresis was observed in the relationship between flow rate and square root pressure difference. The permeability of the exposed permeation cell apparently agrees with that of clean cell activated by treatments of air baking and hydrogen reduction. Similar results on the pressure dependence of the permeability were obtained in the previous runs(M-1-3). Mechanical strength of the cell was enough to be operated at high pressure( 850-940kPa ) and temperature (710K ).

Figure 6 shows the effects of oil vapor exposure( at 713K ) and of activation treatments. Although a marked deterioration of the permeability occurred by contamination with oil vapor, recovery of it was easily performed by air baking( required time was about 30 min at 713K). Permeation coefficient after the treatment agreed with that of clean permeation cell(  $2.7 \times 10^{-7} \text{ mol.cm/cm}^2 \cdot \text{min.kPa}^{1/2}$  ).

## 2.5. Effects of thermal cycling

In order to test the effects of thermal cycling on the permeability and the mechanical strength of a commercial palladium alloy(Pd-Ag.Au.Ru) membrane, permeation characteristics of the membrane during several thermal cyclings were examined. The cyclings were performed in  $\text{H}_2$  gas atmosphere at 390kPa. Permeability was measured at high pressure range

(101 - 973kPa) and high temperature( about 710K). Table 3 and Figure 7-9 show typical experimental results. As shown in the Table and the Figure 7, constant pressure dependence( Sieverts' law ) and constant permeation coefficient were obtained up to high pressure (750 - 970kPa ). In the Figure 8, which shows the permeation flow rate of the permeation cell during cooling, cooling velocity was about 2 degree/min. (716 - 470K) and 0.7 degree/min (470 - 340K). It is noticed that two Arrhenius relations exist in the line drawn against reciprocal temperature. Palladium in the temperature below 473K are considered to form palladium hydrides. Figure 9, which was obtained at 553K, reveals that pressure dependence of permeability is similar to those obtained at high temperature ( about 700K ), and that mechanical strength is maintained.

Through this experimental work, it is proved that the present palladium alloy membrane has high resistivity against thermal cycling in hydrogen atmosphere.

### 3. Design of palladium diffuser

#### 3.1 Operating conditions of diffuser

In design of diffuser, operating temperature and hydrogen concentration in bleed stream from diffuser are important parameters. Although it is easy to produce pure hydrogen isotopes by palladium alloy membrane method, it has a weak point in obtaining bleed stream without hydrogen. In order to attain sufficient recovery of tritium in feed gas, it is necessary to reduce concentration of hydrogen gases in bleed stream as low as possible. The practicable concentration will be determined by evacuation capacity of vacuum pump.

To prevent tritium leak through structural materials of diffuser, operating temperature and driving pressure are desirable to be lowered. As seen in Figure 8, permeability of Pd-alloy membrane varies not so largely in the temperature range of 200°C - 400°C. However, operating temperature should be taken sufficiently higher than the point of formation of palladium hydrides to obtain large and stable permeation coefficient. In present design, 573K(300°C) was selected as operating temperature of diffuser.

Back pressure should be determined by the requirement of hydrogen concentration in bleed  $[H_2]_b$ . It is expressed by partial pressure of hydrogen,

$$[H_2]_b \geq \frac{P[H_2]_p}{P[H_2]_f} \approx \frac{P_L}{P_H}$$

where,  $P[H_2]_p$  and  $P[H_2]_f$  are the hydrogen partial pressure

of permeated stream and feed stream, respectively.  $P_L$  and  $P_H$  are back pressure and driving pressure, respectively.  $P[H_2]_f$  is approximately equal to driving pressure.

Entire concentration of impurities in fusion reactor exhaust gases is assumed to be very low, a few percents at most, so that  $P[H_2]_f$  is approximately equal to total pressure of the exhaust gases. Therefore, to reduce  $[H_2]_b$  to the order of one percent, back pressure must be lowered less than 1/100 of that of driving pressure.

In case of  $P[H_2]_p = P_L \approx 0$  and  $P[H_2]_f \approx P_H$ , hydrogen permeability is proportional to the square root of driving pressure, so that elevating of the pressure is not so effective. For the reason, design value of the driving pressure is taken as 101.3kPa(760Torr),

### 3.2 Analysis of separation characteristics

A mathematical model was formulated to predict the separation characteristics. In multi-tube type Pd-diffuser, hydrogen partial pressure decreases along the diffuser because of permeation. Computer simulation gave partial pressure and permeation flow rate of hydrogen as a function of distance from inlet of the diffuser.

The simulation was made under a few assumptions as follows.

- 1) Pressure and temperature in diffuser do not vary with both the longitudinal position and time.

- 2) Gas contains tritium and unpermeable impurity.
- 3) Radial mixing of gases in diffuser is complete.
- 4) Back pressure is negligible.
- 5) Area of membrane is constant.

Figure 10 shows the mathematical model of diffuser. A flow path in the diffuser was divided into  $N$  elements. Each element was assumed to be a Continuous Stirred Tank Reactor (CSTR), in which flowing gases are mixed perfectly. The material balance equations for the  $n$ -th element are,

$$H_n = H_{n+1} + P_n$$

$$I = I_{n+1} = I_n$$

where,  $H_n$  is the flow rate of hydrogen left the  $n$ -th element,

$I_n$  is the impurity flow rate which is constant along tube,

$P_n$  is the hydrogen flow rate permeated through the  $n$ -th element.

Since permeation obeys Sieverts' law,  $P_n$  is described by

$$P_n = Q A \sqrt{Ph} \sqrt{\frac{H_n}{H_n + I}}$$

where,  $Q$  is the permeation coefficient, and  $A$  is the wall area of an element.

Since the equations were described by finite-difference method, certain boundary conditions were required. The

contents of feed and bleed streams were given as boundary values :

$$\text{Impurity concentration in feed, } \frac{I}{H_{N+1} + I}$$

$$\text{Hydrogen concentration in bleed, } \frac{H_1}{H_1 + I}$$

To avoid difficulties in dealing with nonlinear equation, calculations were performed by iterative procedures.

Constants were taken at conditions of driving pressure ; 760torr (101.3kPa), back pressure ; vacuum, temperature ; 573 K. Assumed tube size was ; 1.6mm O.D., 1.44mm I.D. and 600mm long. Permeation coefficients for hydrogen isotopes are shown in Figure 11. Lines for hydrogen and deuterium are data obtained experimentally by present study, and a line for tritium is determined by the permeability ratio ( $T/H = 1/2.05$ ), which is reported by Fujita et al.<sup>(6)</sup>. Design value of tritium permeation coefficient, that is  $1.03 \times 10^{-7} \text{ mol.cm/cm}^2 \cdot \text{min.kPa}^{1/2}$ , is obtained at 573K.

Figure 12 shows the summary of results for concentration profiles, which was obtained from solutions for  $H_N$ . Parameter  $1/N$  is a measure of longitudinal mixing in diffuser.

The value of  $H_{N+1} + I$  is the feed flow rate, which can be treated with diffuser under the given boundary conditions. Calculation gave the value as a function of tritium concentration in bleed  $[T_2]_b$ . Figure 13 reveals that in order to obtain low  $[T_2]_b$ , giving high recovery ratio of tritium, feed flow rate should be reduced. However, as seen in the Figure, dependence of feed flow rate upon  $[T_2]_b$  and parameter

N is quite small (this fact is very important in design of real diffuser).

Parameter N was estimated to be 120-180 experimentally and numerically for 60cm tube. It is indicated that flow pattern in the diffuser is nearly plug flow. Although some unfavorable effects such as incomplete radial mixing or pressure drop may occur in real diffuser, deviation from present calculations and experiments will not be so large<sup>(7)</sup>.

### 3.3 Specifications of diffuser

Based on the calculations, palladium diffuser which recovers most of hydrogen from gas mixture can be designed. Figure 14 shows an example of the diffuser with Pd-alloy tubes. The number of tubes and flow rates of gases are determined with the inlet conditions of a fuel cleanup system.

Table 4 is the summary of required number of palladium alloy tubes and diffuser size. Parameter N and  $[T_2]_b$  were taken as 60 and 0.01, respectively. A diffuser with 100 tubes is sufficient to purify the gas under feed conditions of TSTA. In order to reduce tritium concentration in bleed to 1%, the bleed flow rate should be regulated, and the back pressure of the diffuser must be also maintained at the order of 0.13kPa.

A few commercial pumps are available for the purpose. Examples are shown in Table 5 and Figure 15.

#### 4. Description of Fuel Cleanup System (FCU)

##### 4.1 FCU system in TSTA

The main functions of the fuel cleanup system for D-T reactor are,

- (1) to remove accumulated impurities from the reactor exhaust gas and neutral beam gas, and
- (2) to recover tritium from tritiated impurities for reuse in the fuel cycle and to minimize tritium release to the environment.

Although variety of process alternatives have been proposed, none has been proven in a continuous operation mode with tritium. Therefore, as shown in Figure 16, a hybrid type of FCU system utilizing hot metal getter beds (HMB) system and cryogenic molecular-sieve beds (MSB) system has been developed in Tritium Systems Test Assembly (TSTA) in Los Alamos Scientific Laboratory. TSTA is a project to develop and demonstrate the processes and equipments necessary for the safe handling of the equimolar mixture of deuterium and tritium planned as the fuel for commercial fusion reactors.

In HMB system, uranium metal is used as getter because of its selective reactivity for various impurities at high temperature. As seen in Table 6, hydrogen gas can be obtained from  $(D,T)_2O$ ,  $N(D,T)_3$ ,  $C(D,T)_4$ . Difficulties in the system are ; permeation of tritium at high temperature, consumption of getter by formation of uranium oxides, carbides and nitrides, furthermore, necessity of cryogenic adsorption bed and its regeneration system to remove Argon.

MSB system is composed of two catalytic oxidisers and one cryogenic molecular-sieve adsorption bed. The primary oxidiser followed by cryogenic adsorption bed is used (450K) to remove free oxygen in the exhaust gas of fusion reactor. The removal of impurities except helium takes place in the adsorption bed (75K). The secondary oxidiser followed by freezer is used for recovery of tritium from regenerated gas of cryogenic adsorption bed. Tritium compounds in the regenerated gas are converted to DTO, CO<sub>2</sub> and N<sub>2</sub>. Tritiated water frozen out in the freezer (160K) is periodically decomposed by hot metal bed or electrolyzer to recover tritium.

#### 4.2 Alternative FCU system with Pd-diffuser

##### (1) D-T reactor exhaust gases

The species and concentrations of impurities in reactor exhaust gases are not known with certainty. In the present design study, following feed conditions are determined by referring to the FCU inlet quantities of TSTA.

(H,D,T) <sub>2</sub>	14.834	mol/hr	(92.3%)
C(H,D,T) <sub>4</sub>	16.071x10 <sup>-3</sup>	"	(0.1%)
N(H,D,T) <sub>3</sub>	16.071x10 <sup>-3</sup>	"	(0.1%)
(H,D,T) <sub>2</sub> O	80.357x10 <sup>-3</sup>	"	(0.5%)
Ar	964.286x10 <sup>-3</sup>	"	( 6% )
He	160.286x10 <sup>-3</sup>	"	( 1% )
total = 16.027 mol/hr			(100%)

## (2) Process description

Figure 17 shows the chemical flow sheet of the alternative FCU system utilizing Pd-diffusers, catalytic oxidiser, freezers and zinc metal beds. The inlet stream of the system is separated into two streams by first Pd-diffuser (driving pressure; 101kPa, back pressure; 0.13kPa, operating temperature; 573K). The one is hydrogen isotopes stream permeated through palladium alloy membrane. This stream contains no impurities, so that it is directly transferred to ISS (cryogenic hydrogen isotope separation process).

Another one is impurity stream with small amount of tritium, which is bled from the diffuser. This stream is treated with catalytic oxidiser followed by freezers to recover tritium from tritiated compounds. That is,  $C(H,D,T)_4$ ,  $N(H,D,T)_3$  and hydrogen are converted to tritiated water and tritium-free gases ( $N_2, CO_2$ ). To avoid explosive reaction in the oxidiser (773K), concentrations of combustible components are reduced by recycling (reflux ratio; 9) the outlet stream of the oxidiser. In the present design, the inlet concentrations of hydrogen, methane and ammonia are 1/10 of that of bleed stream from diffuser.

Tritiated water, subsequently frozen out at 160K, is periodically vaporized and routed to subsystem, which is composed of two zinc metal beds and a small Pd-diffuser (required area of the membrane is 1/100 of that of first diffuser).

The freezer exhaust gases, Ar, He,  $O_2$ ,  $N_2$  and  $CO_2$ , receive

final detritiation in Effluent Tritium Removal System (ERS). The system in JAERI will be constructed with catalytic oxidiser and molecular sieve bed. Assuming the equilibrium vapor concentration at 160K is 0.0013ppm and isotopic ratio of hydrogen(T/D) is 1.0, the amount of tritium exhausted from the freezer is about 12Ci/yr.

Zinc beds in the subsystem are alternately operated to decompose tritiated water by forming stable oxide of zinc. When the capacity of one bed is exhausted, flow is switched to another bed.

Second Pd-diffuser can separate hydrogen from impurities, which are  $\text{CO}_2$  and water vapor passed through the zinc bed.

Because the subsystem is operated in circulation mode, the bleed water can be perfectly decomposed. Therefore, if moderate reaction efficiency per path is achievable in the zinc bed, the operating temperature can be lowered than present design temperature.

When partial pressure of hydrogen comes to 1.3kPa, gases in the subsystem is returned to the inlet of the catalytic oxidiser. Principal impurity is  $\text{CO}_2$ .

In order to evaluate the present system, advantages and disadvantages of alternative FCU systems are summerized in Table 7.

## 5. Conclusion

Feasibility of palladium alloy membrane method was confirmed by experiments. No poisoning was observed in experiments with impurities supposed to be contained in plasma effluent gases. Thermal cycling in hydrogen atmosphere caused neither brittle failure nor distortion of palladium alloy tube.

Computer simulation of palladium diffuser was performed. A multi-tube type diffuser can recover most of hydrogen in reactor exhaust gases. A diffuser with 100 permeation tubes (60cm long) will be able to purify the feed gases of TSTA under condition of 573K, 101kPa.

A design study of fuel cleanup system was made. An alternative FCU system without hot uranium beds and cryogenic molecular-sieve beds becomes available by adopting palladium diffuser. Advantages of the present system are, production of hyper pure hydrogen isotope stream, non-production of uranium wastes, non-necessity of special helium separator.

In the further study, it is necessary to develop such components as catalytic oxidiser, freezer, zinc bed, and to demonstrate whole system in continuous operation mode with tritium.

### Acknowledgement

The authors are grateful to Dr. J. R. Bartlit(LASL), who had been visited to JAERI( 1981.8.4 - 8.28 ), for helpful comments and valuable discussions based on the design philosophy of the TSTA in Los Alamos Scientific Laboratory.

The authors also wish to thank Mr. Matsuda(JAERI), Mr. Kinoshita(JAERI) and Mr. Hirata(Kawasaki Heavy Industry Co, Ltd.) for their advices on computer calculation.

### References

- (1) Anderson, J. L., Sherman, R. H. : " Tritium Systems Test Assembly ", LA-6855-P, (1977).
- (2) " Preliminary Safety Analysis Report for the Tritium Systems Test Assembly ", Los Alamos Scientific Laboratory, University of California, Los Alamos, New Mexico 87545 (1979).
- (3) Kerr, E. C., Bartlit, J. R., Sherman, R. H. : Proc. Tritium Technology in Fission, Fusion and Isotopic Applications, 115(1980).
- (4) Goto, R. : Chemical Economy & Engineering Review, October, 44(1970).
- (5) Yoshida, H., et al. : JAERI-M 9677(1981).
- (6) Fujita, H., et al. : J. Nucl. Sci. Technol., 17, 40 (1980).
- (7) Ackerman, F. J., Koskinas, G. J. : Ind. Eng. Chem. Fundom., 11, 332 (1972).

### Acknowledgement

The authors are grateful to Dr. J. R. Bartlit(LASL), who had been visited to JAERI( 1981.8.4 - 8.28 ), for helpful comments and valuable discussions based on the design philosophy of the TSTA in Los Alamos Scientific Laboratory.

The authors also wish to thank Mr. Matsuda(JAERI), Mr. Kinoshita(JAERI) and Mr. Hirata(Kawasaki Heavy Industry Co. Ltd.) for their advices on computer calculation.

### References

- (1) Anderson, J. L., Sherman, R. H. : " Tritium Systems Test Assembly ", LA-6855-P, (1977).
- (2) " Preliminary Safety Analysis Report for the Tritium Systems Test Assembly ", Los Alamos Scientific Laboratory, University of California, Los Alamos, New Mexico 87545 (1979).
- (3) Kerr, E. C., Bartlit, J. R., Sherman, R. H. : Proc. Tritium Technology in Fission, Fusion and Isotopic Applications, 115(1980).
- (4) Goto, R. : Chemical Economy & Engineering Review, October, 44(1970).
- (5) Yoshida, H., et al. : JAERI-M 9677(1981).
- (6) Fujita, H., et al. : J. Nucl. Sci. Technol., 17, 40 (1980).
- (7) Ackerman, F. J., Koskinas, G. J. : Ind. Eng. Chem. Fundom., 11, 332 (1972).

Table 1 Impurity composition in bleed gas under various flow conditions of permeation cell

Run	flow rate (mol/min)		temperature (K)	pressure** (kPa)	gas velocity (cm/sec)	impurities in feed gas (ppm)					impurities in bleed gas (ppm)						
	feed	bleed				NH <sub>3</sub>	N <sub>2</sub>	CH <sub>4</sub>	O <sub>2</sub>	CO <sub>2</sub>	CO	NH <sub>3</sub>	N <sub>2</sub>	CH <sub>4</sub>	O <sub>2</sub>	CO <sub>2</sub>	CO
I-1	2.8 x10 <sup>-3</sup>	3.7 x10 <sup>-4</sup>	707	356	3.8	10200	+	+	+	+	+	58100	*	*	*	*	
I-2	2.2 "	9.2 "	"	309	4.4	"	"	"	"	"	"	23500	*	*	*	*	
I-3	2.7 "	15.4 "	"	205	8.8	"	"	"	"	"	"	16300	*	*	*	*	
I-4	3.0 "	1.0 "	"	870	1.5	"	"	"	"	"	"	-	1100	+	+	+	
I-5	4.0 "	2.0 "	"	640	2.8	"	"	"	"	"	"	-	640	+	+	+	
I-6	2.1 "	1.1 "	"	320	3.0	"	"	"	"	"	"	-	120	+	+	+	
I-7	1.2 "	0.5 "	"	120	4.3	"	"	"	"	"	"	-	30	+	+	+	
I-8	0.7x10 <sup>-3</sup>	2.2x10 <sup>-4</sup>	"	174	2.4	*	+	1050	1000	-	+	-	+	4940	+	-	+
I-9	1.5 "	9.6 "	"	178	5.9	"	"	"	"	"	"	-	+	2670	20	-	+

+ lower than detection limit of TCD type gas chromatograph using hydrogen carrier gas

- unmeasurable by TCD type gas chromatograph using molecular sieve-5A

\* not detected by TCD type gas chromatograph using chromosorb-103 column

\*\* pressure of permeated hydrogen was kept at 101.3kPa.

Table 2 Experimental conditions and results of methane gas exposure

*1 Run	pre-treatments	permeation temperature (K)	pressure dependence of permeability <sup>*2</sup>	permeation <sup>*3</sup> coefficient	maximum driving pressure ( kPa )
M-1	exposure to CH <sub>4</sub> gas (709K, 30min, 196kPa)	709	Sieverts' law	$2.7 \times 10^{-7}$	850
M-2	" (709K, 16hrs, 134kPa)	709	"	$2.7 \times 10^{-7}$	850
M-3	" (709K, 88hrs, 372kPa)	709	"	$2.7 \times 10^{-7}$	940
M-4	" (823K, 15.5hrs, 382kPa)	703	"	$2.7 \times 10^{-7}$	940

\*1 runs were carried out successively

\*2 operating pressure of permeated hydrogen was kept at 101.3kPa

\*3 unit ;  $\text{mol.cm/cm}^2 \cdot \text{min.kPa}^{1/2}$

Table 3 Experimental conditions and results of thermal cycling in H<sub>2</sub> gas atmosphere

Run*1	pre-treatments	permeation temperature (K)	pressure dependence*2 of permeability	permeation coefficient*3	maximum driving pressure (kPa)
T-1	303 → 703K in vacuum*4	703	Sieverts' law	$2.3 \times 10^{-7}$	775
T-2	698 → 513 → 703K in H <sub>2</sub> gas (393kPa)	703	"	$2.6 \times 10^{-7}$	754
T-3	703 → 380 → 716K " (393kPa)	716	"	$2.7 \times 10^{-7}$	930
T-4	716 → 503 → 713 → 303 → 713K in H <sub>2</sub> gas (393kPa)	713	"	$2.7 \times 10^{-7}$	971
T-5	baking with air (709K, 30min, 101.3kPa)	709	"	$2.7 \times 10^{-7}$	806
T-6	without treatments	553	"	$2.4 \times 10^{-7}$	961

\*1 runs were carried out successively

\*2 operating pressure of permeated hydrogen was kept at 101.3kPa

\*3 unit ;  $\text{mol.cm/cm}^2 \cdot \text{min.kPa}^{1/2}$ 

\*4 permeation cell had been kept under vacuum for about 3 months

Table 4 Diffuser size, number of tubes and flow rate

shell diameter $D_i$ (mm)	Pd-tube diameter $d$ (mm)	pitch $s$ (mm)	number of Pd-tubes $N(-)$	flow rate $F$ (mol. $T_2$ /hr)
18	1.6	3.2	24	4.87
31	"	"	76	15.4
37	"	"	100	20.3
52	"	"	200	40.6

$d$  ; outer diameter

$D_i$  ; inner diameter ,  $D_i = [s(\sqrt{69 + 12N - 3})/3] + d$

$F$  ; at  $P_h=101.3\text{kPa}$ ,  $P_l=0.133\text{kPa}$ ,  $T=573\text{K}$ , permeability for  $T_2$

$Q = 1 \times 10^{-7}$  (mol.cm/cm<sup>2</sup>.min.kPa<sup>1/2</sup>)

Table 5 Specifications of S.R.T.I. pumps

TYPE	PBT-124	PBT-135	PBT-105
number of cylinders	5	4	3
number of stages	4	5	5
minimum intake pressure(Torr)*	1	0.7	0.7
intake flow rate(m <sup>3</sup> /hr)	4.5	15	8.1
maximum exhaust pressure(bars)	15	5	5

\* exhaust pressure = 760 Torr

Table 6 Reactivity of uranium metal

Reactant	Reaction Temperature (°C)	Products
H <sub>2</sub>	250	α-and β-UH <sub>3</sub>
N <sub>2</sub>	700	UN , UN <sub>2</sub>
O <sub>2</sub>	150-350	UO <sub>2</sub> , U <sub>3</sub> O <sub>8</sub>
H <sub>2</sub> O	100	UO <sub>2</sub>
NH <sub>3</sub>	700	UN
CH <sub>4</sub>	635-900	UC
CO	750	UO <sub>2</sub> +UC
CO <sub>2</sub>	750	UO <sub>2</sub> +UC

Table 7 System evaluation

systems	advantages	disadvantages
present system with Pd-diffuser	<ul style="list-style-type: none"> <li>◦ produce hyper pure hydrogen</li> <li>◦ no He separator is required</li> <li>◦ continuous operation in main stream with one diffuser</li> </ul>	<ul style="list-style-type: none"> <li>◦ operating temperature of diffuser is comparatively high (573 K)</li> <li>◦ requires recovery system for tritiated impurities</li> <li>◦ replacement of zinc metal beds</li> </ul>
cryogenic adsorption with catalytic oxidation	<ul style="list-style-type: none"> <li>◦ low temperature in main stream operation</li> </ul>	<ul style="list-style-type: none"> <li>◦ requires regeneration system, and recovery system for tritiated impurities</li> <li>◦ little data on tritium inventory at low temperature</li> </ul>
hot metal getters followed by cryogenic adsorption	<ul style="list-style-type: none"> <li>◦ no recovering system for tritiated impurities</li> </ul>	<ul style="list-style-type: none"> <li>◦ requires cryogenic adsorption bed for inert gas (Ar)</li> <li>◦ permeation and materials problems at high temperature (1170 K)</li> <li>◦ replacement of uranium getter beds</li> <li>◦ uranium metal waste</li> </ul>

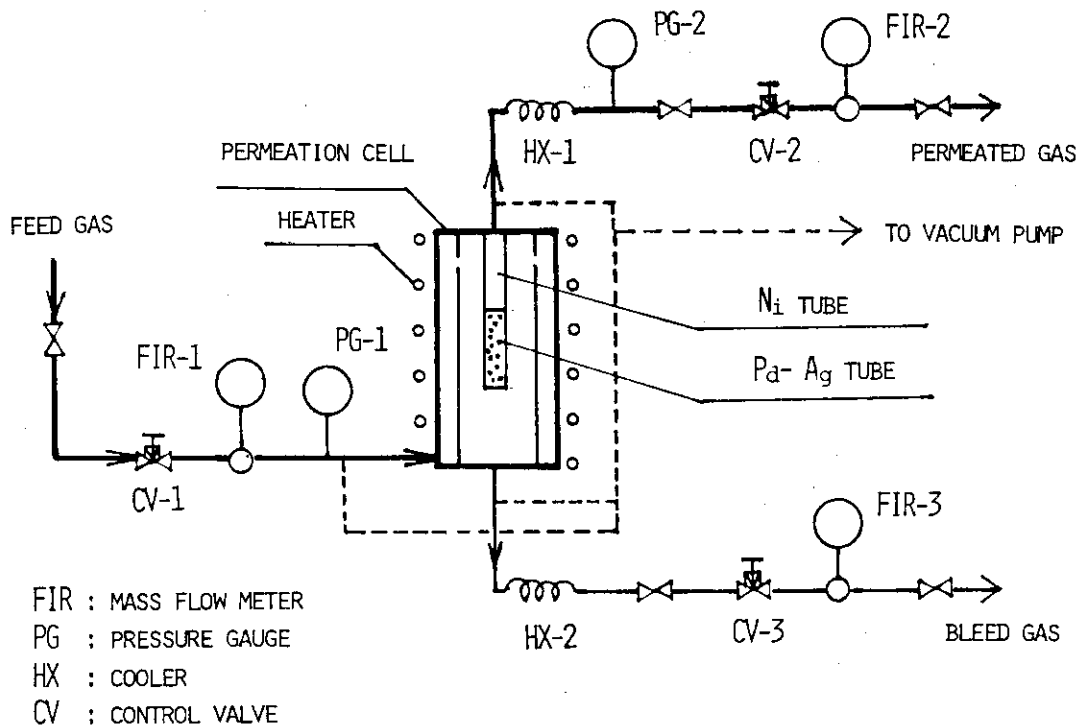


Fig. 1 Conceptual flow sheet of experimental apparatus

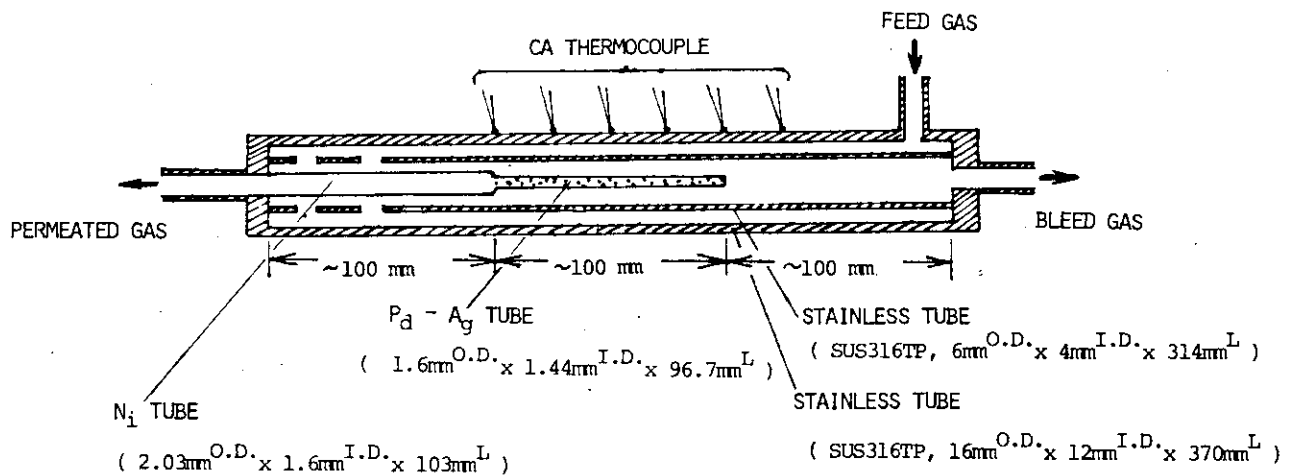


Fig. 2 Detail structure of permeation cell

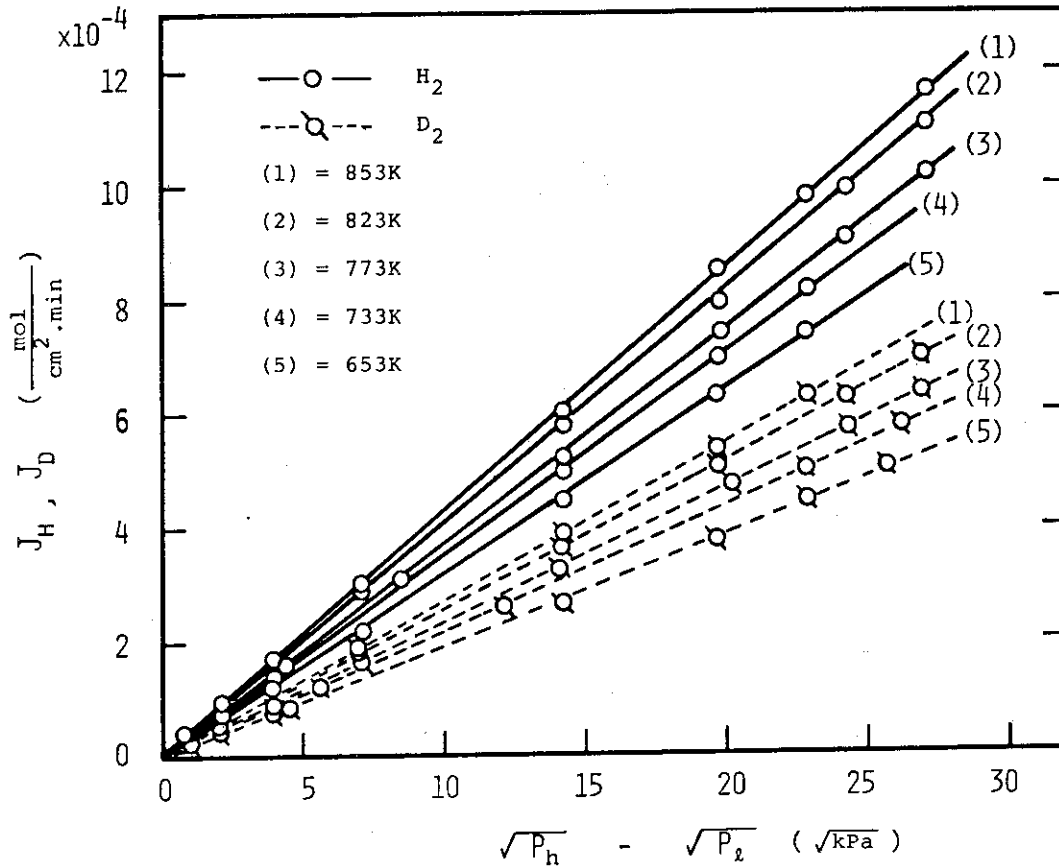
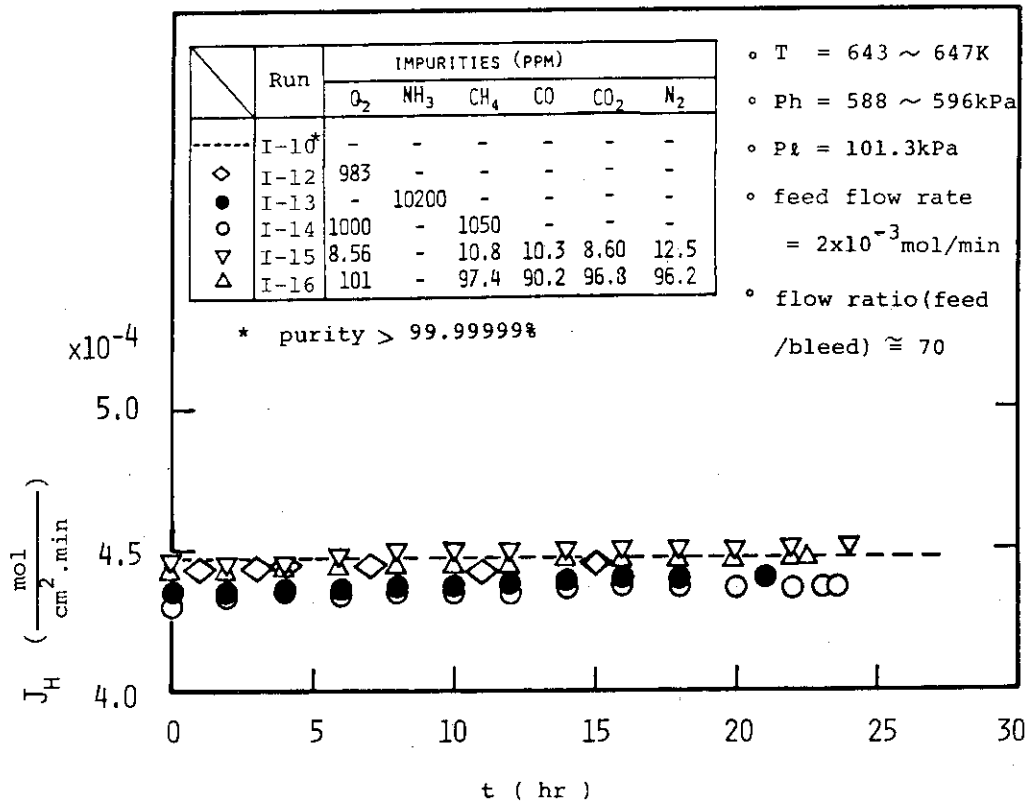
Fig. 3 Basic permeability for H<sub>2</sub> and D<sub>2</sub>

Fig. 4 Effects of impurities on hydrogen permeability

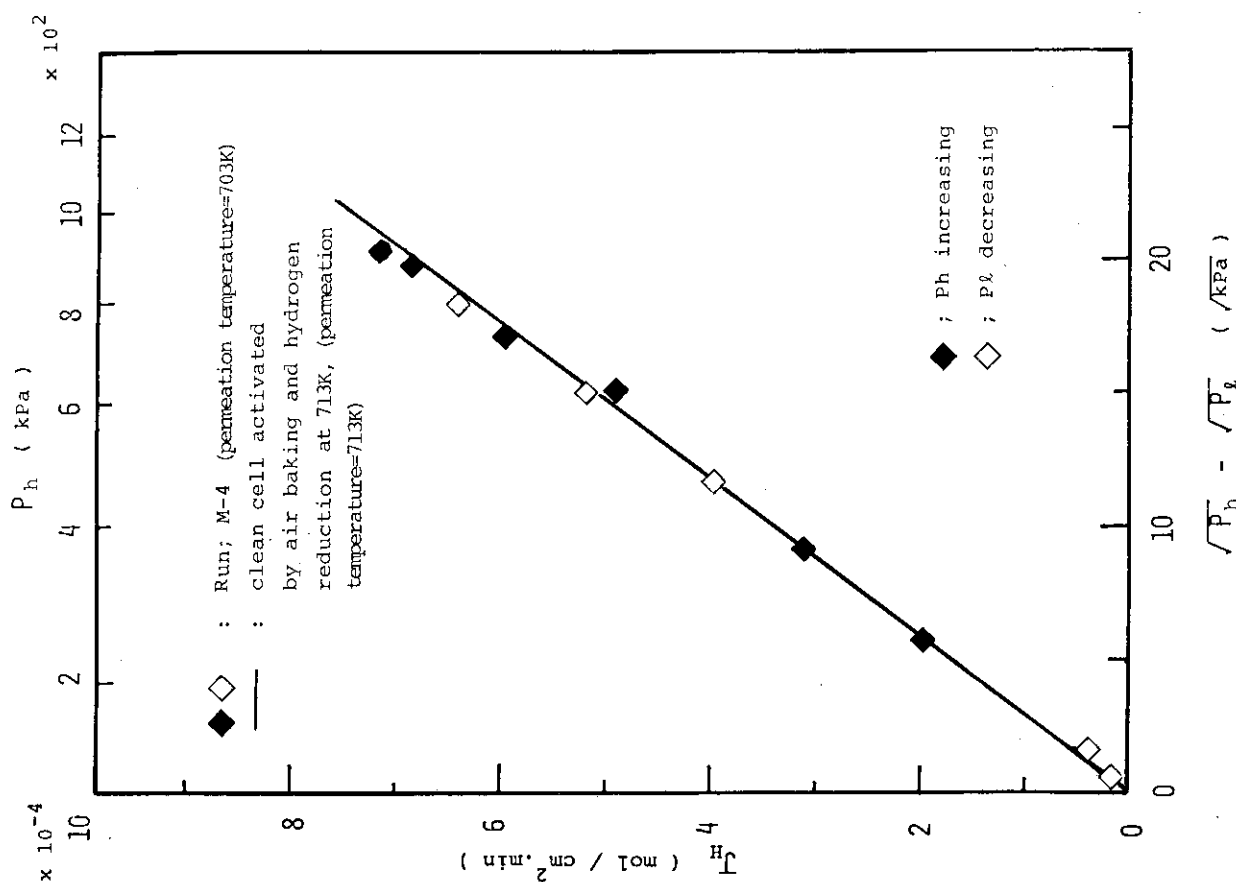


Fig. 5 Effects of methane gas exposure on hydrogen permeability

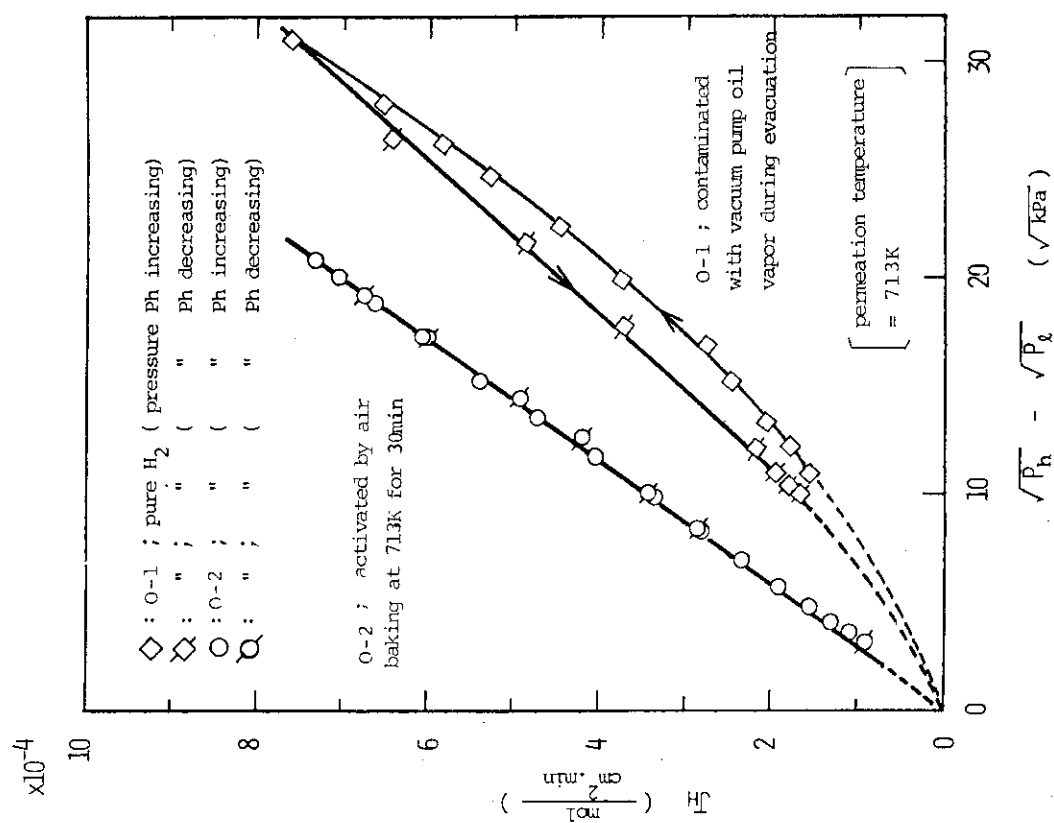


Fig. 6 Effects of oil vapor exposure on hydrogen permeability

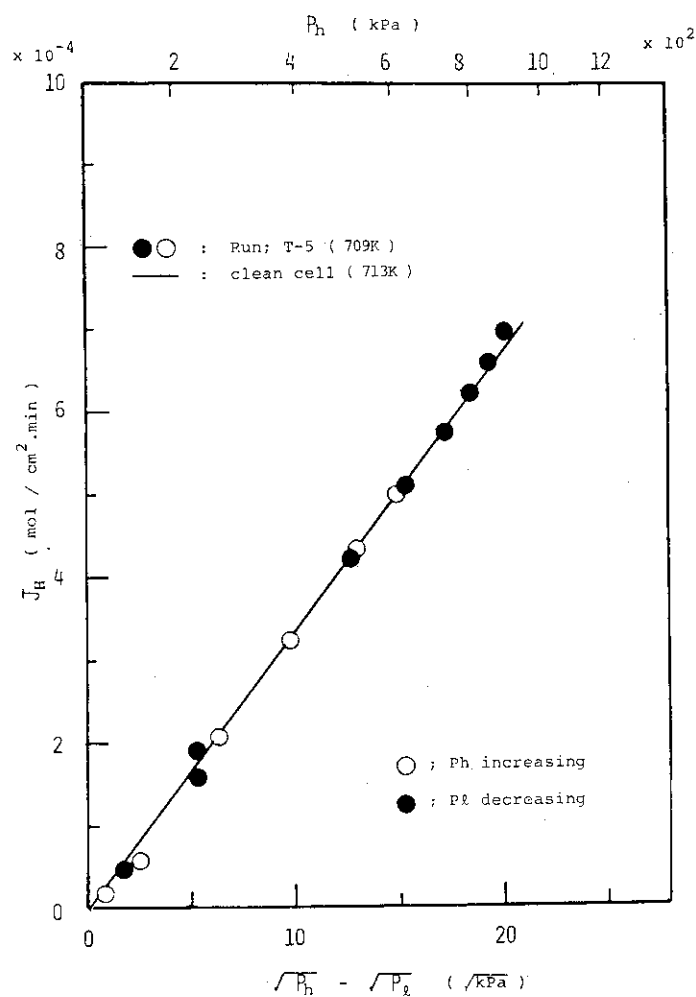


Fig. 7 Effects of thermal cycling on hydrogen permeability

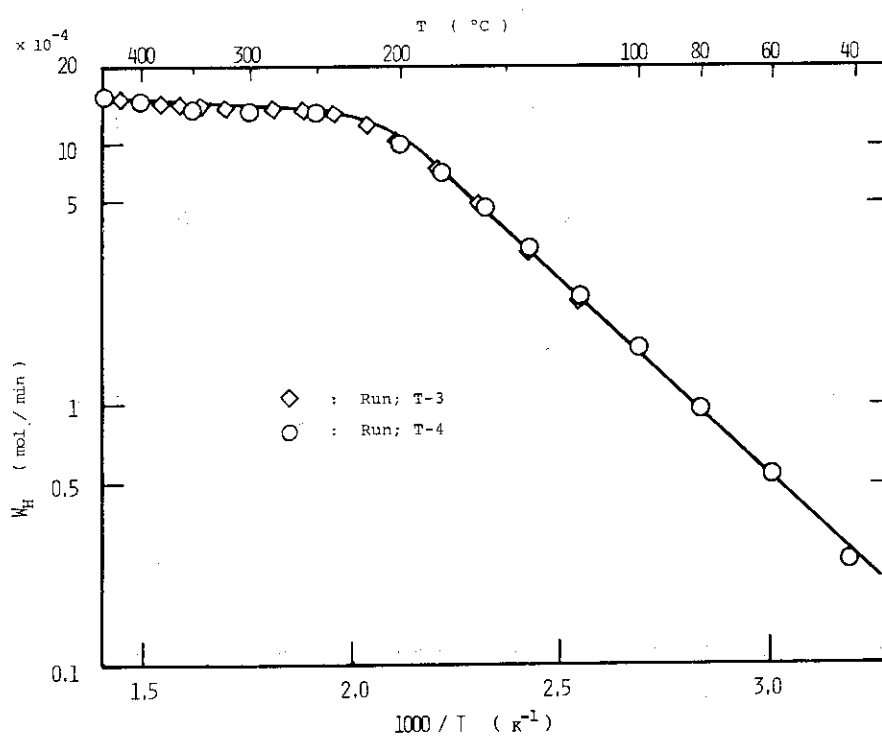


Fig. 8 Permeability during cooling down

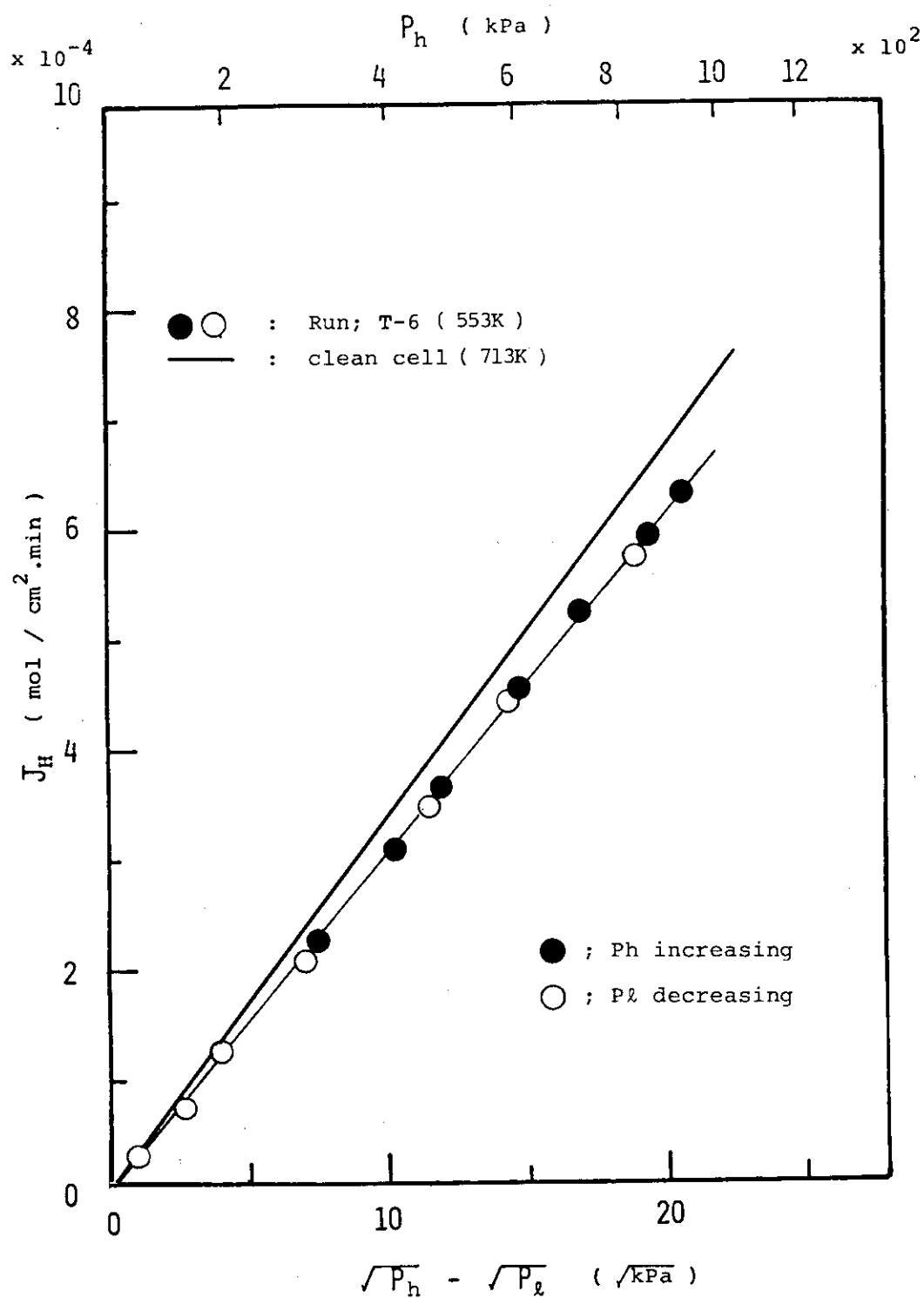


Fig. 9 Permeability at comparatively low temperature (553K)

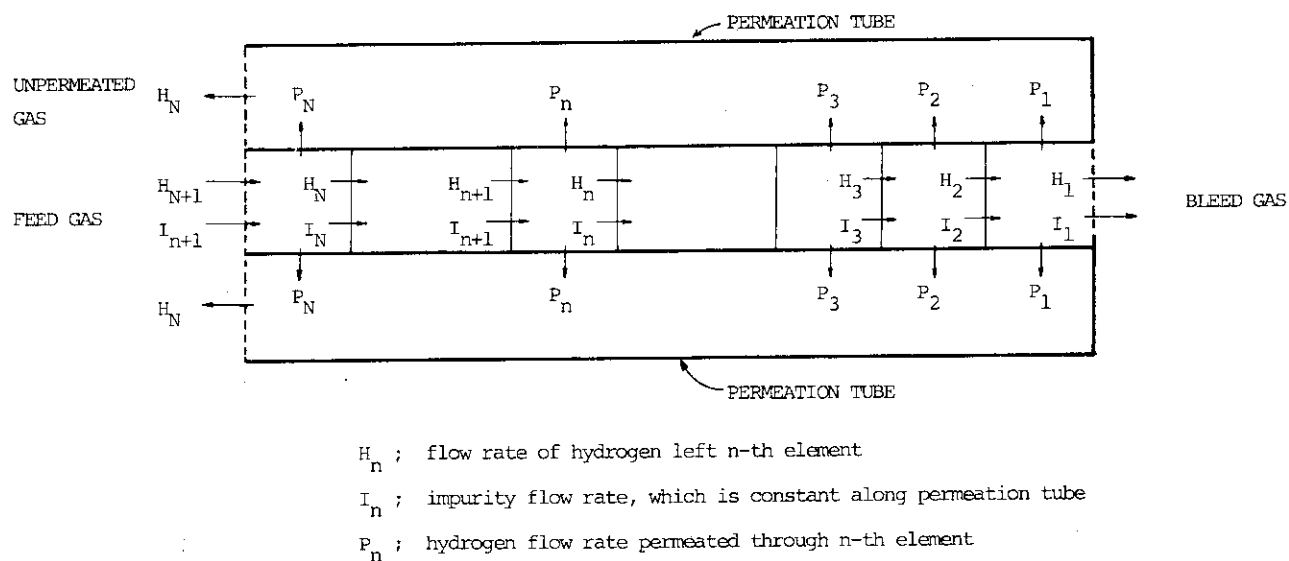
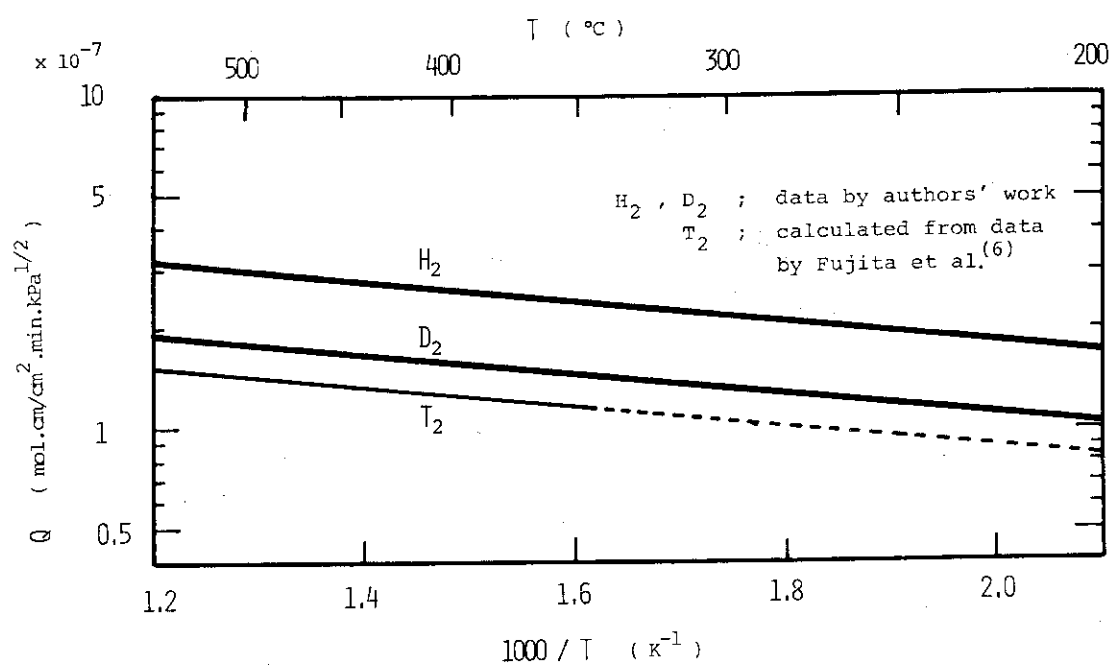


Fig. 10 Mathematical model of Pd-diffuser

Fig. 11 Temperature dependence of permeation coefficient for  $H_2$ ,  $D_2$  and  $T_2$

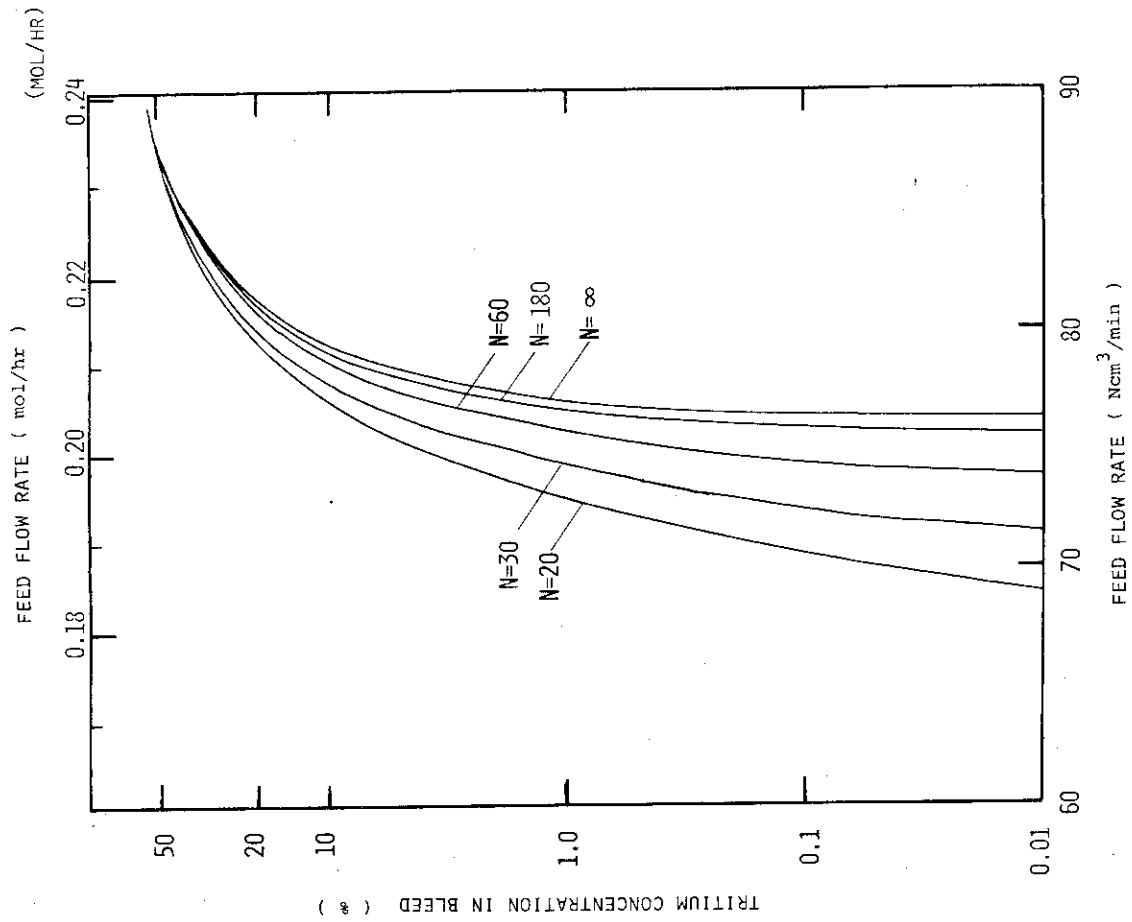


Fig. 12 Hydrogen concentration profiles in Pd-diffuser

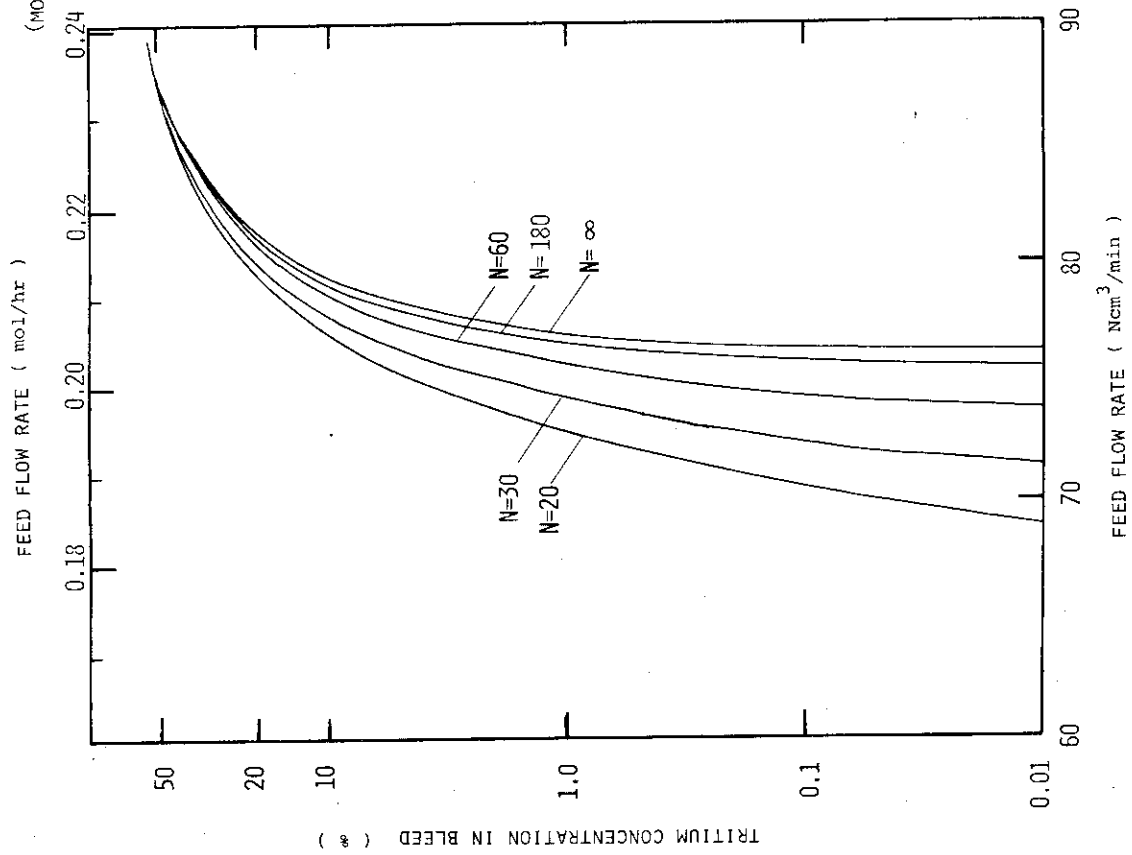


Fig. 13 Tritium concentration in bleed stream against feed flow rate

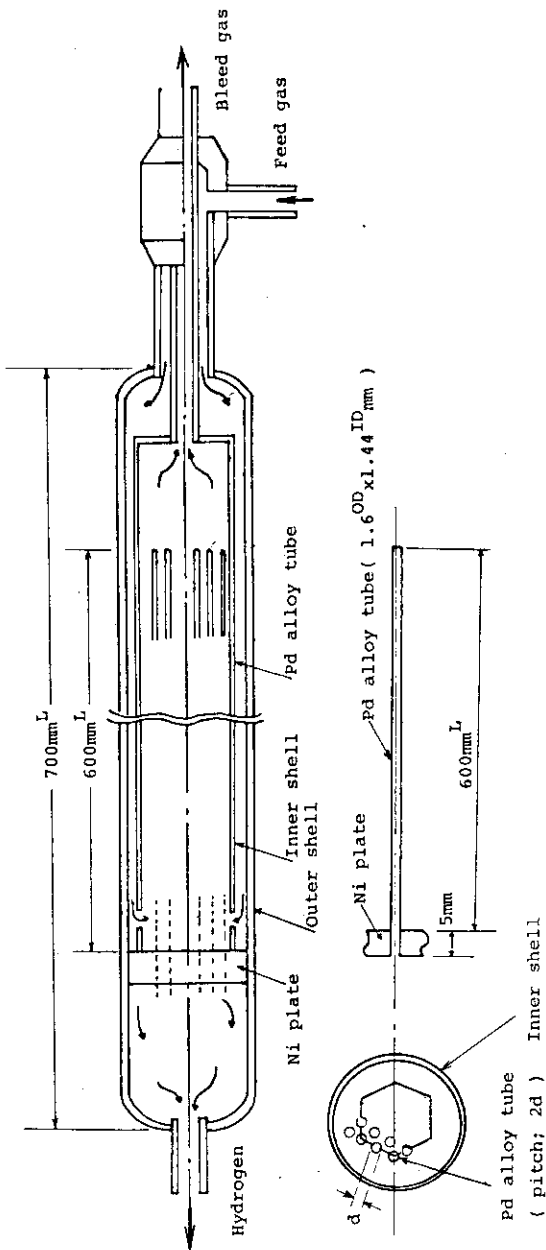


Fig. 14 Structure of multi-tube type Pd-diffuser

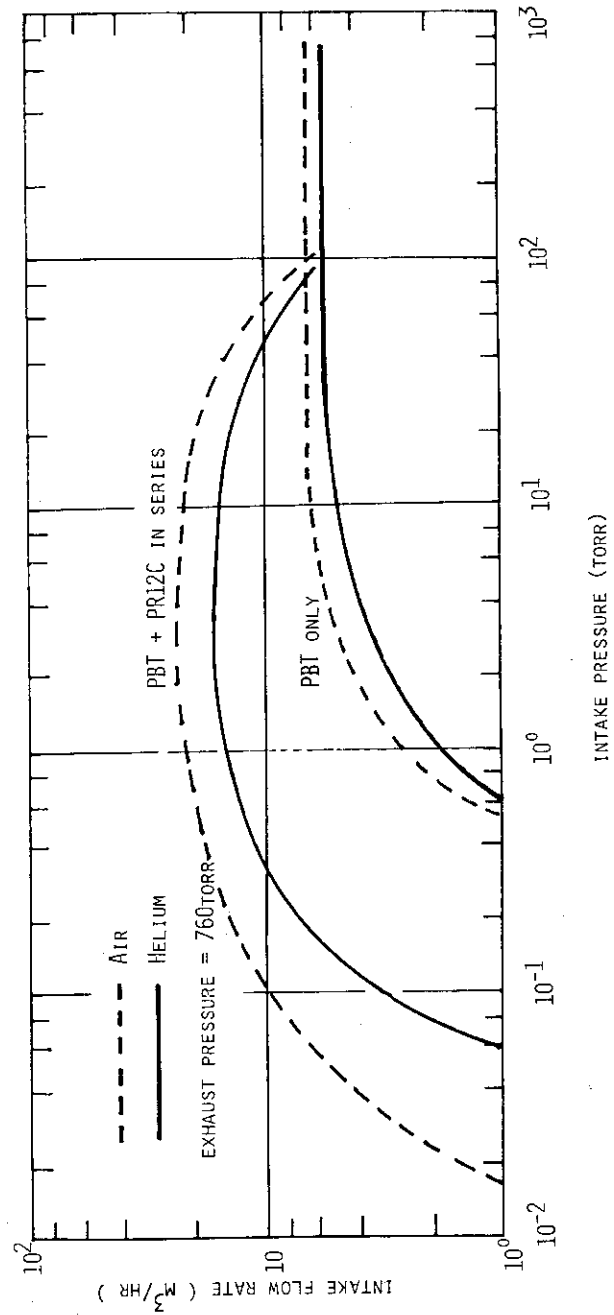
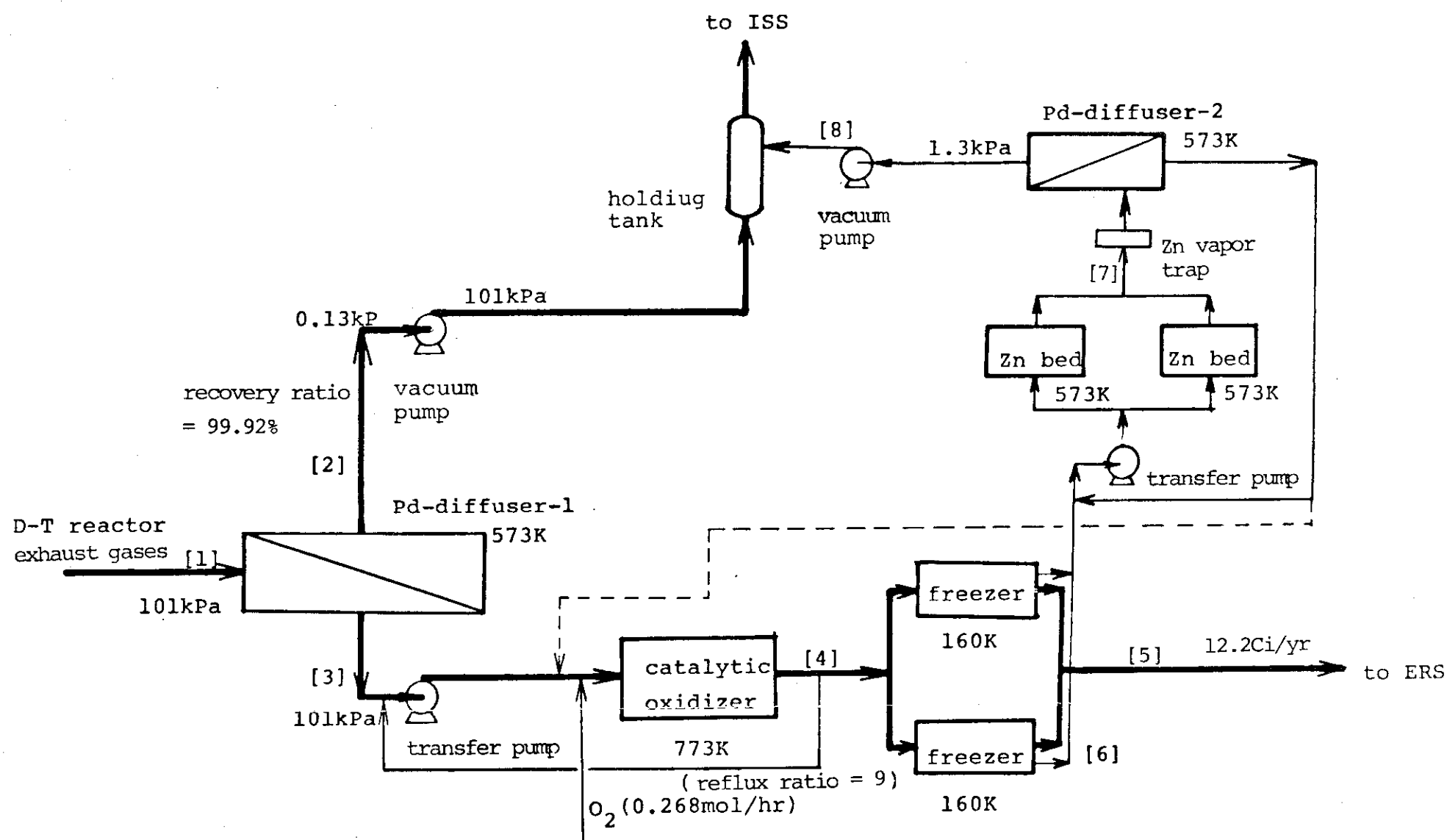


Fig. 15 Performance of S.R.T.I. pumps





species	[1]	[2]	[3] *1	[4] *2	[5]	[6] *4	[7] *5	[8] *6
Hydrogen	14.834 mol/hr (92.3%)	14.822 mol/hr	12.375x10 <sup>-3</sup> mol/hr (1%)	12.375x10 <sup>-9</sup> mol/hr	12.375x10 <sup>-9</sup> mol/hr	-	-	3.279 mol/day
C(H,D,T) <sub>4</sub>	16.071x10 <sup>-3</sup> (0.1%)	0	16.071x10 <sup>-3</sup> (1.3%)	16.071x10 <sup>-9</sup>	16.071x10 <sup>-9</sup>	-	-	0
N(H,D,T) <sub>3</sub>	16.071x10 <sup>-3</sup> (0.1%)	0	16.071x10 <sup>-3</sup> (1.3%)	16.071x10 <sup>-9</sup>	16.079x10 <sup>-9</sup>	-	-	0
(H,D,T) <sub>2</sub> O	80.357x10 <sup>-3</sup> (0.5%)	0	80.357x10 <sup>-3</sup> (6.4%)	148.981x10 <sup>-3</sup>	1.777x10 <sup>-9</sup> *3	3.279 mol/day	-	0
Ar	964.286x10 <sup>-3</sup> (6%)	0	964.286x10 <sup>-3</sup> (77.1%)	964.286x10 <sup>-3</sup>	964.286x10 <sup>-3</sup>	-	-	0
He	160.714x10 <sup>-3</sup> (1%)	0	160.714x10 <sup>-3</sup> (12.9%)	160.714x10 <sup>-3</sup>	160.714x10 <sup>-3</sup>	-	-	0
O <sub>2</sub>	0	0	0	217.617x10 <sup>-3</sup>	217.617x10 <sup>-3</sup>	-	-	0
N <sub>2</sub>	0	0	0	8.036x10 <sup>-3</sup>	8.036x10 <sup>-3</sup>	-	-	0
CO <sub>2</sub>	0	0	0	16.071x10 <sup>-3</sup>	16.071x10 <sup>-3</sup>	-	-	0

- \*1 chemical reactions in palladium diffuser were neglected  
 \*2 reduction ratios for hydrogen, methane and ammonia were assumed as 1/10<sup>6</sup>  
 \*3 equilibrium vapor concentration at 160K was assumed as 0.0013ppm  
 \*4 depends on adsorption amounts of each species on the surface of freezer

- \*5 depends on design condition of freezer and Zn bed  
 \*6 when partial hydrogen pressure comes to 1.3kPa, bleed gas is transferred to inlet of catalytic oxidizer  
 \*7 isotopic ratio (T/D) was assumed as 1.0

Fig. 17 Chemical flow sheet of alternative FCU system with Pd-diffuser